Progress In Electromagnetics Research C, Vol. 72, 197–205, 2017

Ultra-Small Single-Negative Metamaterial Insulator for Mutual Coupling Reduction of High-Profile Monopole Antenna Array

Yujie Qiu[1, 2, *], Lin Peng[1], Xing Jiang[1], Zhuzhu Sun[1], and Shaoyu Tang[1]

Abstract—A novel single-negative magnetic (SNG) metamaterial (MTM) insulator is designed to reduce mutual coupling between high-profile monopole antennas. As a kind of metamaterials, the proposed SNG MTM-resonator utilized concentric rings embedded complementary metal structures. Then, an insulator is achieved with a highly compact structure. The band-gap of the insulator is attributed to the negative permeability of the magnetic resonance. A well-engineered MTM-resonator is then embedded in between a high-profile monopole antenna array for coupling reduction. The antenna array is designed, fabricated, and measured. Both numerical and experimental results indicate a mutual coupling reduction of more than 17 dB. The 20 dB isolation bandwidth about 16% is obtained. The proposed prescription with electrically small dimensions and high decoupling efficiency opens an avenue to new types of high-profile antennas with super performances.

1. INTRODUCTION

Electromagnetic mutual coupling or interference between closely spaced antenna array elements is a major cause of performance degradation [1]. In recent years, reduction of mutual coupling techniques has been studied for physically small arrays, e.g., by using the EM band-gap structures (EBG) [2–5] and even by incorporating the resonant slits or defects in the ground [6, 7]. However, most of the insulating structures are large, resulting in a big element separation for antenna applications.

In recent years, the unique characteristics of single-negative (SNG) metamaterial (MTM) have attracted much attention and provide a conceptual route for mutual coupling suppression of array [8–16]. In [8–13], the SNG MTM-insulators were proposed for mutual coupling suppression in low-profile planar antenna array. In [11], a single-negative magnetic metamaterial insulator was designed and then applied in the closely-spaced high-profile monopole antennas with a high decoupling efficiency. However, the design in [11] has only 200 MHz operating bandwidth (-10 dB). Although this method markedly reduces separation between array elements along y-direction, the SNG MTM-insulator has a large size in x-direction ($0.73\lambda_0$ at the operating wavelength in [11]).

In this paper, a novel SNG MTM-insulator is shown to be an effective design for reducing mutual couple in high-profile antenna array elements. The proposed MTM-insulator that uses the single-negative magnetic MTM-inspired resonator is electrically smaller ($0.26\lambda_0 \times 0.26\lambda_0 \times 0.02\lambda_0$ in x-, z- and y-directions, and λ_0 is the free space wavelength at 5 GHz). Therefore, the proposed design is smaller than [11] in x-direction. The technique can provide an isolation improvement of more than 17 dB between two closely spaced monopole elements (with a distance of $0.5\lambda_0$). Compared to [11], the compact SNG MTM-insulator proposed in this paper has a broadband performance, and the isolation bandwidth 20 dB reaches 16% relative to the center frequency 5 GHz. The design is fabricated and measured.

Received 8 October 2016, Accepted 25 March 2017, Scheduled 5 April 2017

* Corresponding author: Yujie Qiu (qiuyjie@163.com).

[1] School of Information and Communication, Guilin University of Electronic Technology, Guilin, Guangxi 541004, China. [2] School of Electronic and Optical Engineering, Nanjing University of Science and Technology, Nanjing, Jiangsu 210094, China.

2. DESIGN AND ANALYSIS OF THE MTM-RESONATOR

2.1. Structure and Constitutive Effective Parameters Analysis

For characterization and design, the commercial full-wave finite method (FEM) EM field simulator Ansoft HFSS is employed. Figure 1 shows the front view of the unit cell geometry of the proposed SNG MTM-resonator structure which consists of one square-shaped conductive layer on a dielectric substrate. The conductive layer consists of the complementary ring metallic structure (CRMS), the complementary gear-type metallic structure (CGMS) and ring structures (RSs). As shown in the figure, the CRMS and CGMS are embedded inside with each other, and the center ring structures (RSs) comprise one split ring and one complete ring interconnected by four small strips. The Arlon AD260A substrate (relative permittivity $\varepsilon_r = 2.6$ and dielectric loss tangent $\tan\delta = 0.0017$) with a thickness of 1 mm is used in this research. The top layer is made up of copper with conductivity of 5.8×10^7 S/m and a thickness of 0.035 mm. The SNG MTM-resonator parameters defined in Figure 1 are $a = 16$ mm, $b = 15$ mm, $r_1 = 7$ mm, $r_2 = 6$ mm, $r_3 = 2$ mm, $g_1 = 0.5$ mm, $g_2 = 0.3$ mm, and $w_1 = 0.4$ mm.

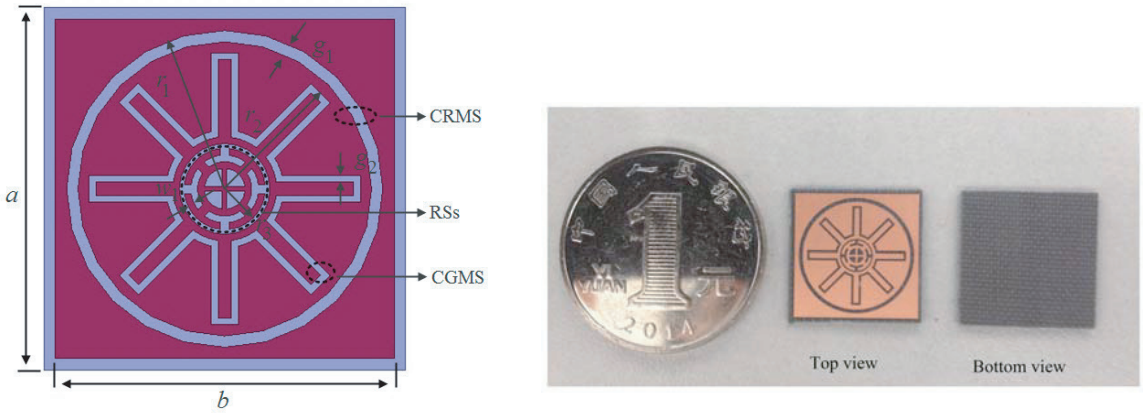

(a) (b)

Figure 1. Proposed SNG MTM-resonator topology. (a) Dimensional parameters. (b) View photograph of the fabricated prototype.

In order to analyze the characteristics of the proposed SNG MTM-resonator, two EM simulation models are set up as shown in Figure 2. For the driven mode analysis in Figure 2(a), a perpendicularly incident transverse electric and magnetic (TEM) plane wave (along x-direction) with a polarized electric field in the z-direction is considered for the calculation of the scattering parameters of the MTM-resonator structure. With the assignment of periodic boundary conditions on the single unit-cell of Figure 2(a), the transmission characteristics of the resonator (reflection and transmission coefficients) are obtained as shown in Figure 2(b). Referring to Figure 2(b), the transmission dip center at 5 GHz is clearly observed corresponding to the magnetic resonance of MTM-resonator.

Based on the results, the retrieval method in [17] has been used for extracting the effective medium parameters. Figure 2(c) shows the effective permittivity and permeability of the SNG MTM-resonator. As ? expected, it is observed that the negative permeability metamaterial exhibits a strong the magnetic resonance behavior at around 5 GHz. In addition, the severe shock in the effective permittivity parameters at 5.7 GHz is observed corresponding to the electric resonance of MTM-resonator. Therefore, from Figure 2(b), the jitter in the reflection and transmission coefficients around 6 GHz is attributable to the electric resonance of the resonator when impinges to the axial E-field of the incoming wave. The slight discrepancies are attributable to the computation tolerances induced by the meshing variations.

2.2. Dispersion Diagram Analysis

For further characterization, the dispersion curves β are cautiously computed from the eigen-mode analysis performed in HFSS. In this process, the EM simulation of the structure can be carried out

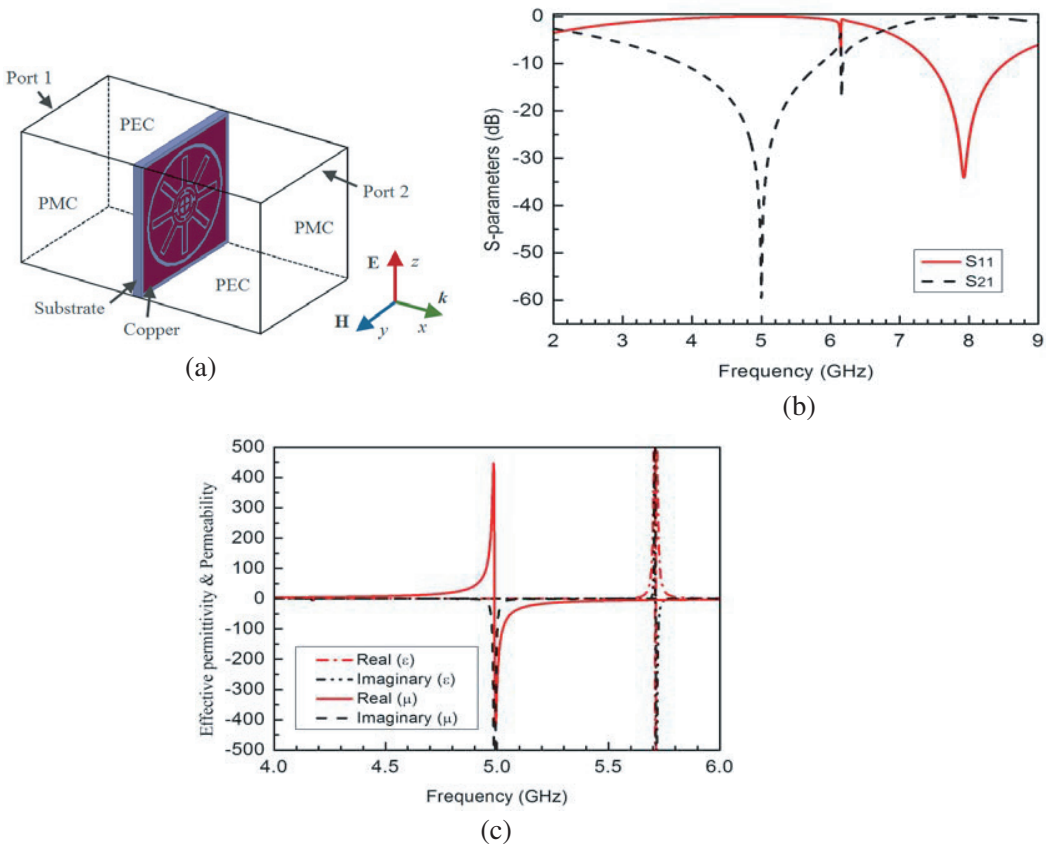

Figure 2. Analysis of the proposed SNG MTM-resonator. (a) Simulation setup for driven mode analysis in HFSS, (b) EM Simulated S-parameters and (c) retrieved effective permittivity and permeability of the proposed SNG MTM-resonator unit cell shown in Figure 1.

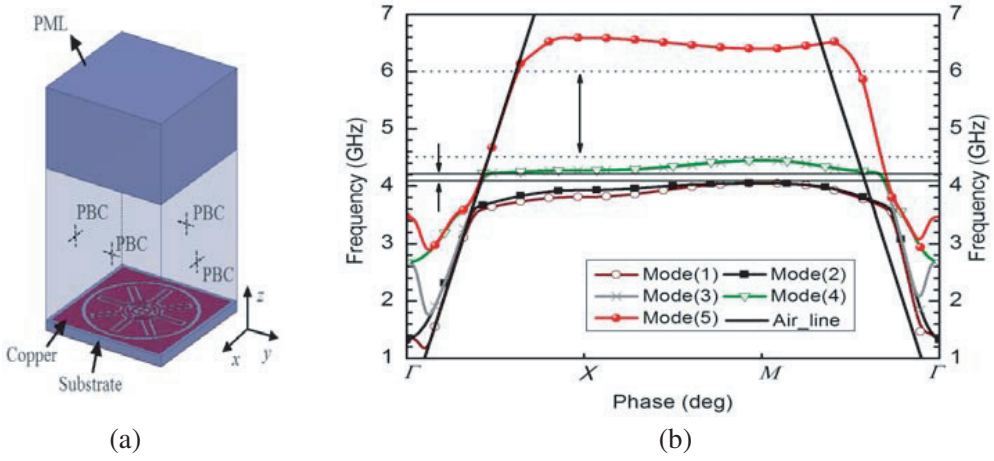

Figure 3. (a) Simulation setup for eigenmode analysis in HFSS as well as (b) dispersion diagram of the proposed SNG MTM-resonator unit cell.

through assigning the periodic boundary condition (PBC) to the four planes parallel to the x- and y-directions with the perfectly matched layer (PML) condition perpendicular to the horizontal plane (xoy plane) as shown in Figure 3(a). The dispersion diagram in the $\Gamma - X$ section of the full Brillouin Zone is plotted in Figure 3(b). As expected, two band-gaps are clearly evidenced from 4.1 to 4.2 GHz

and 4.52 to 6 GHz, respectively. Therefore, compared to Figures 2(b) and (c), the indicated band-gaps coincide well with the band of SNG permeability characterized from driven mode analysis previously. Furthermore, if β is close to the air line in the lower band, the propagation mode couples strongly with the air mode, resulting in a sharp transition.

3. MUTUAL COUPLING REDUCTION OF HIGH-PROFILE MONOPOLE ANTENNA ARRAY

One of the most important and promising applications of SNG MTM-insulator should be the capability to suppress EM mutual coupling of a closely spaced antenna array at frequencies located in the band-gap region. To demonstrate the efficient decoupling characteristic of the proposed SNG MTM-insulator in high-profile monopole antenna array, a monopole antenna array is proposed as shown in Figure 4. The array has two elements with an optimized separation of $d = \lambda_0/2$, where λ_0 is the wavelength corresponding to the resonant frequency of monopole antenna. The two antennas have been designed to operate at a frequency of 5 GHz. A finite copper ground plane of size $2.5\lambda_0 \times 2.5\lambda_0$ is used. In addition, the model setup for the monopole antennas is fabricated using two brass rods of length 25 mm and diameter of 1.3 mm, soldered to 50 Ω coaxial (SMA) connectors. The proposed SNG MTM-insulator formed by only one single MTM-resonator is aligned vertically between the two monopole antennas to reject the interaction of the elements. The size of insulator in x- and z-directions is $0.26\lambda_0 \times 0.26\lambda_0$. For verification, the MTM-insulator loaded monopole antenna array is fabricated as shown in Figure 4(b).

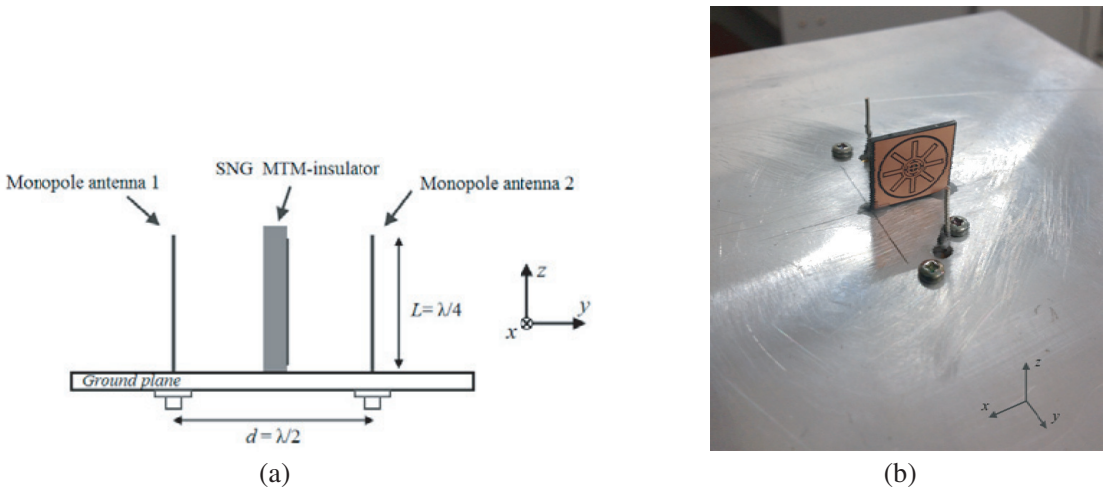

Figure 4. Topology of the proposed monopole array using SNG MTM-insulator. (a) Side view of schematic of the proposed antenna. (b) Photograph of the fabricated prototype.

The S-parameters versus different values of d are plotted in Figure 5. The simulation results show that as d decreases, due to the mutual coupling between the antenna and insulator, the return losses of two antennas deteriorate, and the isolation band shifts to the lower region. Therefore, there exists a trade-off between the return losses of the antenna and mutual coupling reduction, and d should be selected according to the actual demand.

In order to validate the mutual coupling reduction performance of the proposed approach, a prototype with $d = \lambda_0/2$, as shown in Figure 4(b), is fabricated and measured. The two-port antenna systems with and without the insulator are both measured by an N5230A vector network analyzer with their measured and simulated results plotted in Figure 6 for comparison. Figure 6(a) presents the results of the reference array (without insulator), and Figure 6(b) demonstrates the results of the proposed array (with insulator). As shown in the figures, good consistency of the simulated and measured reflection S_{11} and transmission S_{21} coefficients is observed for the arrays. Figure 6(a) shows the simulated and measured S_{11} of the referenced array. Simulated result indicates that -10 dB operation bandwidth

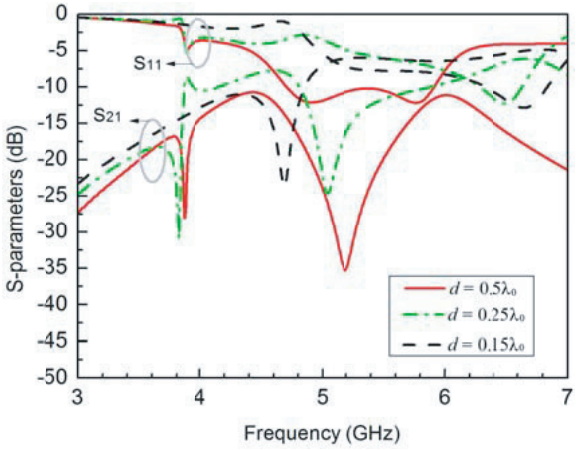

Figure 5. The S-parameters of the proposed monopole array, with different values of d.

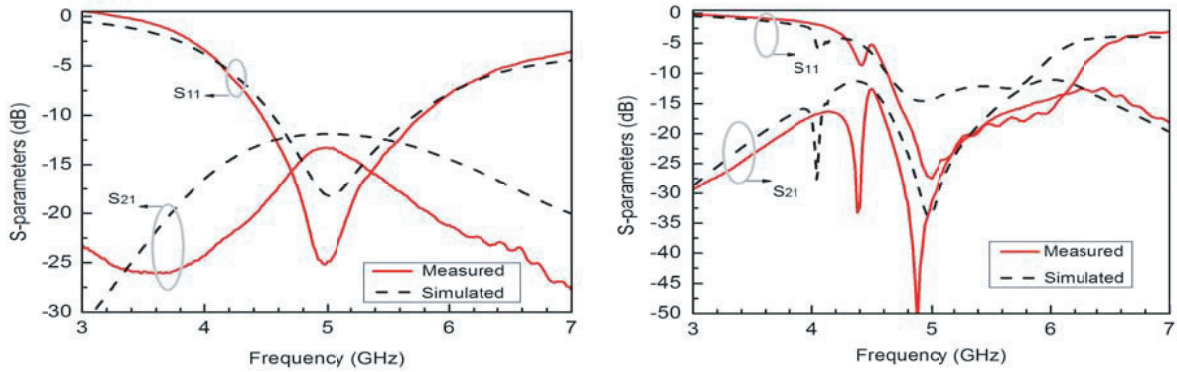

Figure 6. Comparisons of the reflection and transmission coefficients of the (a) reference and (b) SNG MTM-insulator-loaded antenna between simulation and measurement.

covers from 4.5 to 5.8 GHz. The measured result agrees well with the simulated one. The simulated and measured S_{21} of the reference array indicate the mutual coupling of -11 dB and -13 dB at resonance frequency (5 GHz), respectively. For the proposed array, the comparison between the simulated and measured S_{11} is shown in Figure 6(b). It is seen that the 10 dB return loss bandwidth ranges from 4.6 to 6 GHz for the simulated result and from 4.6 to 6.3 GHz for the measured one. Both the simulated and measured mutual couplings (S_{21}) at 5 GHz are about -30 dB. The corresponding 20 dB isolation bandwidths are 4.7–5.4 GHz and 4.6–5.4 GHz, respectively.

The measured and simulated S_{11} are better than -10 dB in both cases, indicating a good impedance match for the two-antenna system. An exciting inspection from S_{21} indicates that the coupling for the two monopoles has been significantly suppressed at 5 GHz, e.g., the peak S_{21} is measured on the order of -13 dB for reference antenna, whereas it is drastically reduced to -30 dB for the proposed antenna. Note that the mutual coupling (S_{21}) is lower than -10 dB without decoupling structures, and it is a not bad isolation for the monopole array. However, a mutual coupling reduction of 17 dB has been realized, while at same time the 20 dB isolation bandwidth is over 16% for the MTM-loaded antenna.

To examine the band-gap behavior on the radiation performances, the gain patterns of both the reference monopole element (without insulator) and proposed element (with insulator) are calculated in HFSS. Notice that the antenna performances are evaluated under the condition of one-port excitation (element radiation behavior not array behavior). The simulated radiation patterns for both xoy- and yoz-planes at 5 GHz are plotted in Figure 7. From Figure 7(a), for xoy-plane, it is seen that the proposed monopole element is almost identical to the reference case. Following Figure 7(b), it is observed that

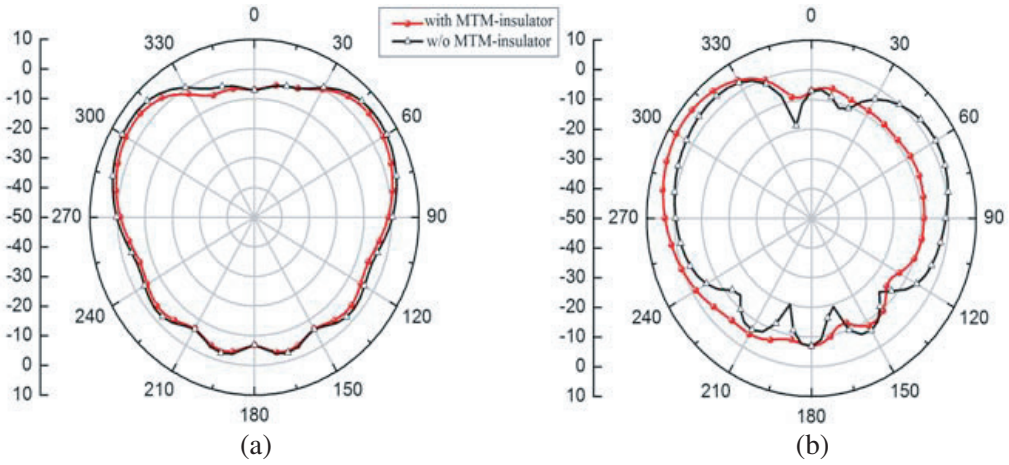

Figure 7. Comparisons of calculated gain patterns for the monopole element with and without SNG MTM-insulator at 5 GHz in two principle planes: (a) *xoy*-plane. (b) *yoz*-plane.

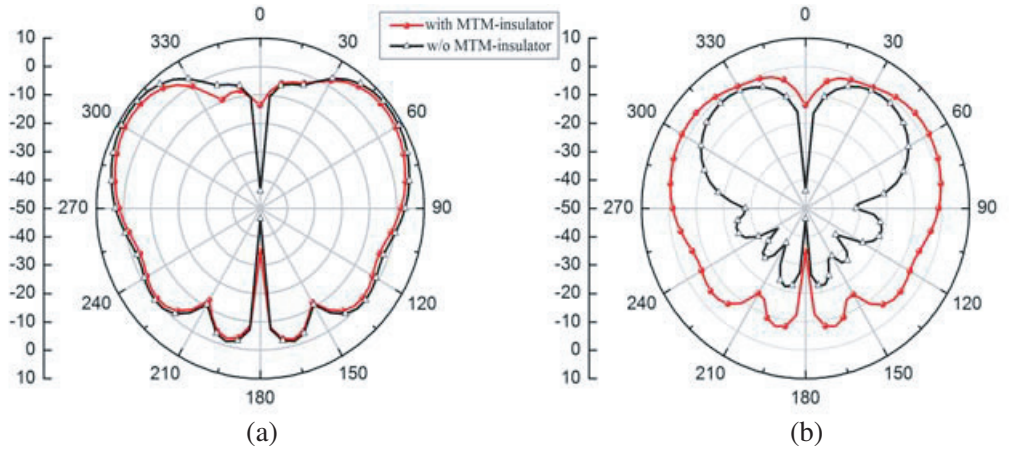

Figure 8. Comparisons of calculated gain patterns for the monopole array with and without SNG MTM-insulator at 5 GHz in two principle planes: (a) *xoy*-plane. (b) *yoz*-plane.

the use of SNG MTM-insulator enhances the proposed element's potential to steer or concentrate energy into a more specified direction (*y*-direction), thus increasing the gain in specified directions, whereas the reference element yields a typical donut shape. This is expected as MTM-insulator, which is perpendicular to the *yoz* plane, affects the *yoz*-plane of radiation pattern. Therefore, the gain has increased from 6.2 dB for the reference monopole element case to 7.4 dB for the MTM-insulator-loaded element.

Figure 8 shows far-field patterns for the reference and proposed arrays (without and with insulator) at 5 GHz (array behavior). Unsurprisingly, for *xoy*-plane, the proposed array is consistent with the reference array as shown in Figure 8(a). However, it is observed that radiation pattern of the proposed array in *yoz*-plane is different from the reference case in Figure 8(b). The far-field pattern of the proposed insulator-loaded array in *yoz*-plane has a donut shape as that in *xoz*-plane. It is because the radiation patterns of elements of the proposed array in *yoz*-plane have been changed as elucidated previously in Figure 7(b). Therefore, the proposed array achieves quasi-orthogonal patterns (*xoz*-plane and *yoz*-plane) when using the SNG MTM-insulator. Due to the nature of the SNG MTM-insulator losses, the gain of the MTM antenna array drops to 7.5 dB compared to reference array (8.8 dB).

The calculated efficiencies of the reference and proposed arrays (without and with insulator) are shown in Figure 9. It can be observed that when the insulator is inserted, the fluctuation of the array

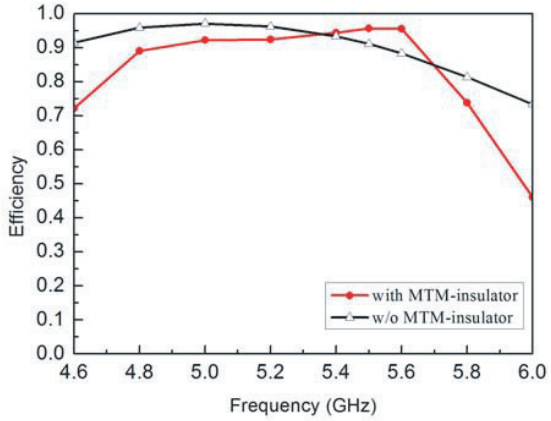

Figure 9. Comparisons of calculated efficiencies for the monopole array with and without SNG MTM-insulator.

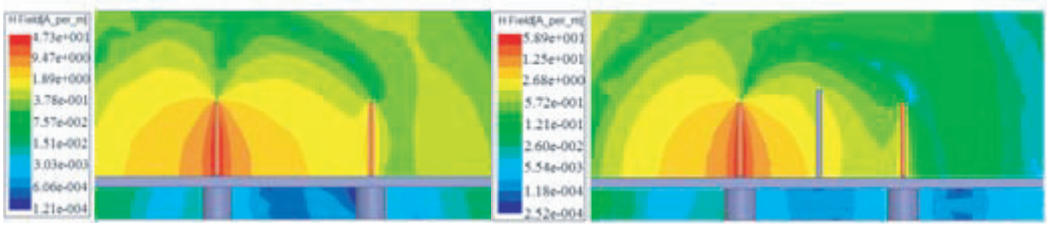

Figure 10. Simulated H field distribution. (a) Reference antenna. (b) MTM-antenna.

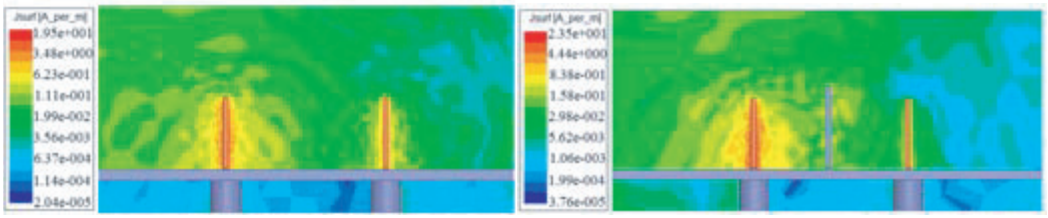

Figure 11. Simulated current distribution. (a) Reference antenna. (b) MTM-antenna.

efficiency is very small in the operation band (4.8 GHz–5.8 GHz). At 5 GHz, the total efficiency is close to 97.1% for the reference array,and decreases a little (the efficiency of 92.2%) for the proposed one. Note that the SNG MTM-insulator is used in the design, and it deteriorates the total efficiency outside of the operation band as shown in Figure 9. Despite this, the results of MTM-antenna do not show any additional significant differences and notable changes at the operating frequency with the effective suppression of element mutual coupling.

To make deep insight into the insulator loaded array, the HFSS-simulated magnetic field distribution and current distribution for the array with one antenna transmitting and the other receiving are shown in Figure 10 and Figure 11, respectively. From Figure 10(a), the horizontal magnetic field generated from the excitation element propagates through the space and produces the mutual coupling to the receiving element. When incorporating with the SNG MTM-insulator as in Figure 10(b), the horizontal magnetic field is rejected by the insulator. As shown in Figure 11, the usage of the insulator also abates the current inspired in the receiving element. Then, coupling between the elements can be effectively reduced by the proposed insulator.

4. CONCLUSION

This paper presents a novel strategy to design a compact SNG MTM-insulator with a broad bandgap and high decoupling efficiency. Comprehensive analysis of the proposed MTM-resonator is performed. The insulator formed by the resonator, the fabricated prototype of size $0.26\lambda_0 \times 0.26\lambda_0 \times 0.02\lambda_0$, is applied in the high-profile monopole array. The resultant antenna makes advance in many aspects such as the mutual coupling reduction of more than 17 dB, the 20 dB isolation bandwidth of 16% and easy fabrications. The effective coupling reduction of the proposed insulator indicates that it is a good candidate in high-profile antenna array applications.

ACKNOWLEDGMENT

This work was supported in part by National Natural Science Foundation of China (Grant Nos. 61401110 & 61371056), and in part by Natural Science Foundation of Guangxi (Grant No. 2015GXNSFBA139244).

REFERENCES

1. Hansen, R. C., *Phased Array Antennas*, Ch. 7, Wiley, New York, 1998.
2. Cai, T., G.-M. Wang, J.-G. Liang, and Y.-Q. Zhuang, "Application of ultra-compact single negative waveguide metamaterial for a low mutual coupling patch antenna array design," *Chin. Phys. Lett.*, Vol. 31, No. 8, 0841011–0841015, 2014.
3. Xu, H. X., G.-M. Wang, and M.-Q. Qi, "Hilbert-shaped magnetic waveguided metamaterials for electromagnetic coupling reduction of microstrip antenna array," *IEEE Trans. Magn.*, Vol. 49, No. 4, 1526–1529, 2013.
4. Xu, H.-X., G.-M. Wang, M.-Q. Qi, and H.-Y. Zeng, "Ultra-small single-negative electric metamaterial for electromagnetic coupling reduction of microstrip antenna array," *Opt. Exp.*, Vol. 20, No. 20, 21968–21976, 2012.
5. Bait-Suwailam, M. M., M. S. Boybay, and O. M. Ramahi, "Electromagnetic coupling reduction in high-profile monopole antennas using single-negative magnetic metamaterials for MIMO applications," *IEEE Trans. Antennas Propag.*, Vol. 58, No. 9, 2894–2910, 2007.
6. Sarabandi, K. and Y. J. Song, "Subwavelength radio repeater system utilizing miniaturized antennas and metamaterials channel isolator," *IEEE Trans. Antennas Propag.*, Vol. 59, No. 7, 2683–2691, 2011.
7. Jiang, X., Y.-J. Qiu, and L. Peng, "Novel metamaterial insulator for compact array isolation," *International Conference on Signal Processing, Communications and Computing*, 649–652, Guilin, Guangxi, CN, Aug. 2014.
8. Buell, K., H. Mosallaei, and K. Sarabandi, "Metamaterial insulator enabled superdirective array," *IEEE Trans. Antennas Propag.*, Vol. 55, No. 4, 1074–1085, 2007.
9. Hsu, C. C., K. H. Lin, and H. L. Su, "Implementation of broadband isolator using metamaterial-inspired resonators and a T-shaped branch for MIMO antennas," *IEEE Trans. Antennas Propag.*, Vol. 59, No. 10, 3936–3939, 2011.
10. Yang, F. and Y. Rahmat-Samii, "Microstrip antennas integrated with electromagnetic band-gap (EBG) structures: A low mutual coupling design for array applications," *IEEE Trans. Antennas Propag.*, Vol. 51, No. 10, 2936–2946, 2003.
11. Assimonis, S. D., T. V. Yioultsis, and C. S. Antonopoulos, "Computational investigation and design of planar EBG structures for coupling reduction in antenna applications," *IEEE Trans. Magn.*, Vol. 48, No. 2, 771–774, 2012.
12. Chung, Y., S. S. Jeon, D. Ahn, et al, "High isolation dual-polarized patch antenna using integrated defected ground structure," *IEEE Microwave and Wireless Components Letters*, Vol. 14, No. 1, 4–6, 2004.
13. Chiu, C.-Y., C.-H. Cheng, R. D. Murch, and C. R. Rowell, "Reduction of mutual coupling between closely-packed antenna elements," *IEEE Trans. Antennas Propag.*, Vol. 55, No. 6, 1732–1738, 2007.

14. Chen, X., T. M. Grzegorczyk, B.-I. Wu, J. Pacheco, and J. A. Kong, "Robust method to retrieve the constitutive effective parameters of metamaterials," *Phy. Rev. E*, Vol. 70, 016608, 2004.
15. Imbert, M., P. J. Ferrer, J. M. González-Arbesú, and J. Romeu, "Assessment of the performance of a metamaterial spacer in a closely spaced multiple-antenna system," *IEEE Antennas and Wireless Propagation Letters*, Vol. 11, 720–723, 2012.
16. Dadgarpour,A., B. Zarghooni, and T. A. Denidni, "Mutual-coupling suppression for 60 GHz MIMO antenna using metamaterials," *IEEE International Symposium on Antennas and Propagation & USNC/URSI National Radio Science Meeting*, 2015.
17. Ferrer, P. J., J. M. González-Arbesú, and J. Romeu, "Bidirectional metamaterial separator for compact antenna systems," *IEEE Antennas and Propagation Society International Symposium*, 2007.